Advanced Steel Construction – Vol. 19 No. 2 (2023) 143–149
DOI:10.18057/IJASC.2023.19.2.6

HIGH PRECISION IDENTIFICATION METHOD OF MASS AND STIFFNESS MATRIX FOR SHEAR-TYPE FRAME TEST MODEL

Jin-Peng Tan [1, 2] and Dan-Guang Pan [1, *]

[1] *Department of Civil Engineering, University of Science and Technology Beijing, Beijing 100083, China*
[2] *Huachengboyuan Engineering Technology Group Co., Beijing 100052, China*
* *(Corresponding author: E-mail: pdg@ustb.edu.cn)*

A B S T R A C T

In the direct method of identifying the physical parameters of the shear-type frame structures through the frequencies and modes from the experimental modal analysis (EMA), the accuracy of the lumped mass depends on the initial mass, while the identified mass matrix and stiffness matrix are prone to generate some matrix elements without any physical meaning. In this paper, based on the natural frequencies and modes obtained from the EMA, an iterative constrained optimization solution for correcting mass matrix and a least squares solution for the lateral stiffness are proposed. The method takes the total mass of the test model as the constraint condition and develops an iterative correction method for the lumped mass, which is independent of the initial lumped mass. When the measured modes are exact, the iterative solution converges to the exact solution. On this basis, the least squares calculation equation of the lateral stiffness is established according to the natural frequencies and modes. Taking the numerical model of a 3-story steel frame structure as an example, the influence of errors of measured modes on the identification accuracy is investigated. Then, a 2-story steel frame test model is used to identify the mass matrix and stiffness matrix under three different counterweights. Numerical and experimental results show that the proposed method has good accuracy and stability, and the identified mass matrix and stiffness matrix have clear physical significance.

A R T I C L E   H I S T O R Y

Received: 22 April 2022
Revised: 21 July 2022
Accepted: 27 July 2022

K E Y W O R D S

Shear-type frame;
Test model;
Physical parameter identification;
Mass matrix;
Stiffness matrix

1. Introduction

Shear-type steel frame structure is one of the most common engineering structures. In order to make the designed structure safer and more economical, a lot of theoretical research [1, 2] and experimental research [3, 4] have been carried out. When the stiffness of the beam is much greater than that of the column, this type of structure can be simplified into a lumped mass shear model. In the construction process of actual structures, there are usually geometric errors, material property errors and uncertainty of joint stiffness [5]. After careful consideration of the geometric similarity ratio of the experimental model, the size of the designed experimental model is typically small. As a result, the geometric error of the experimental model has a more significant impact on the mass and stiffness of the structure. In order to predict the response accurately for the analytical model under dynamic load or the damage in different test stages, it is necessary to identify the high precision mass matrix and stiffness matrix of the test model.

Depending on whether a priori model is required, the identification methods of mass and stiffness matrices can be classified as direct methods and indirect methods [6]. The indirect methods are to optimize the parameters of the analysis model to minimize the errors between the calculation results and the experimental results through the model updating method. The objective function of the optimization analysis significantly affects the results of the model updating. Since the frequencies and modes in practical engineering are the most easily obtained parameters, the objective function parameters are often constructed based on frequencies, modes and their derived variables [7-9]. Frequency response functions [10, 11] and time histories [12] contain more high frequency signals and are commonly used to construct objective functions. The iterative calculation of nonlinear equations is involved in the model updating, and the computational workload is considerably large. To improve the computational efficiency, based on sensitivity analysis [13], the nonlinear equations are linearized for the iterative calculation to accelerate the convergence, or artificial intelligence algorithms [14, 15] are used to compute the solution of the optimization equation. This method is suitable for complex large-scale structures and has a wider applicable range, but the computational workload is still significant. The direct methods are to calculate the mass and stiffness matrices of the system directly from the modal parameters or dynamic response time history of the structure without prior finite element model [16]. Among them, the physical parameter identification method based on modal parameters has been widely used because of its simplicity. Berman [17] established the Lagrange multiplier method for mass matrix correction with the minimum modified mass as the objective function. Baruch [18] also used the Lagrange multiplier method to obtain the correction of the mass matrix and stiffness matrix. Wei [19, 20] established methods to update the mass and stiffness matrices simultaneously and studied the interaction influence of mass and stiffness correction. Lee and Eun [21, 22] took the modified mass matrix and stiffness matrix as the objective function, modified the mass matrix and stiffness matrix at the same time and compared the accuracy of different methods to identify the stiffness matrix when the mass matrix was known. Qi [23] established the least squares solution of the lumped mass and lateral stiffness of a shear frame structure under the assumption that the mass and stiffness distribution of each layer is known. For the lumped-mass shear model, if the mass matrix of the system is known, then the stiffness matrix can be calculated directly by inverse analysis of the Jacobi matrix eigenproblem [24].

The direct method is easy to use and is usually suitable for structures with fewer degrees of freedom. Since the frame test model of the lumped mass shear model has fewer degrees of freedom, the mass matrix is diagonal, and the stiffness matrix is tridiagonal, it is more appropriate to use the direct method for calculation. The lumped mass shear model [25] of the frame structure is a simplified computational model obtained by using kinematic constraints. The diagonal matrix formed by the lumped mass is a simplification of the uniform mass matrix. Therefore, the exact value of the lumped mass is unknown. In addition, the calculated length of the column cannot be accurately estimated in the lateral stiffness calculation, which leads to a significant difference between the measured dynamic characteristics of the analytical model and the test model [26, 27]. When the mass matrix is unknown, the direct method to identify the physical parameters of the shear frame structure will face the following problems: (1) The accuracy of the direct method to identify the lumped mass is related to the initial solution, even if there is no modal error, the exact solution of the mass matrix still cannot be obtained. (2) The sparsity of the original matrix cannot be kept in the identified mass matrix and stiffness matrix, that is, the identified mass matrix and stiffness matrix may become full matrices and lose their physical meaning.

To address the above two problems, this paper proposes an iterative constrained optimization solution to correct the mass matrix so that the identified mass matrix is independent of the initial solution and converges to the accurate solution under the accurate mode. After the mass matrix is identified, the least squares solution of the lateral stiffness is also proposed. In this manner, the identified mass matrix and stiffness matrix are kept sparse, and each parameter meets the requirements of the calculation model and has a physical meaning. On this basis, the numerical simulation method was used to identify the mass matrix and stiffness matrix of a three-story frame structure. The influence of the initial mass and errors of measured modes on the identification results were analyzed. Then, the physical parameter identification of a two-story frame test model was studied. Finally, the accuracy and effectiveness of the proposed method are verified by comparing and analyzing the identification results of lumped mass and lateral stiffness of the model under different counterweights.

2. Iterative constrained optimization solution for correcting lumped mass

The N-layer shear frame structure shown in Fig. 1 can be simplified into a lumped mass shear model with N degrees of freedom. When the mass matrix is unknown, the initial lumped mass matrix is assumed to be:

$$\boldsymbol{M}_0 = diag[m_{i,0}] \tag{1}$$

in which $m_{i,0}$ is the lumped mass at the 0th iteration; $\boldsymbol{M}$ is $N\times N$ diagonal mass matrix.

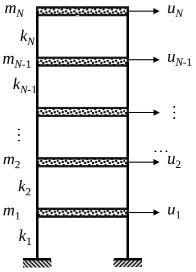

Fig. 1 Calculation model of shear-type frame structure

To identify the mass matrix of the model by the frequency domain method, the natural frequencies of the model and the corresponding modes $\omega_i, \boldsymbol{\phi}_i$ (i=1,2,…,N) are measured from the experimental model analysis. By using the iterative method to correct the mass matrix, the lumped mass matrix and the correction matrix of the (k-1)th iteration are denoted as $\boldsymbol{M}_{k-1}$ and $\Delta\boldsymbol{M}_{k-1}$ respectively, and the corrected mass matrix $\boldsymbol{M}_k$ can be therefore expressed as:

$$\boldsymbol{M}_k = \boldsymbol{M}_{k-1} + \Delta\boldsymbol{M}_{k-1} \tag{2}$$

Normalizing the measured modes gives:

$$\boldsymbol{\phi}_i^{\mathrm{T}}\boldsymbol{M}_k\boldsymbol{\phi}_i = 1 \tag{3}$$

Then

$$\boldsymbol{\phi}^{\mathrm{T}}\boldsymbol{M}_k\boldsymbol{\phi} = \boldsymbol{M}_{B,k} \tag{4}$$

in which $\boldsymbol{\phi}$ is the mode matrix made up of the N modes $\boldsymbol{\phi}_i$. If $\boldsymbol{M}_{B,k}$ is a unit matrix, the modes are orthogonal on $\boldsymbol{M}_k$, and there is no need to correct the mass matrix; otherwise, it needs to be corrected. Let the correction mass matrix $\Delta\boldsymbol{M}_k$ be a diagonal matrix $\Delta\boldsymbol{M}_k = diag[\Delta m_{i,k}]$ so that the corrected mass satisfies:

$$\boldsymbol{\phi}^T(\boldsymbol{M}_k + \Delta\boldsymbol{M}_k)\boldsymbol{\phi} = \boldsymbol{I} \tag{5}$$

where $\boldsymbol{I}$ is the unit matrix. Substituting Eq. (4) into Eq. (5) yields:

$$\boldsymbol{\phi}^{\mathrm{T}}\Delta\boldsymbol{M}_k\boldsymbol{\phi} = \boldsymbol{I} - \boldsymbol{M}_{B,k} \tag{6}$$

Expanding each upper triangular element in Eq. (6) yields:

$$\boldsymbol{\phi}_i^{\mathrm{T}}\Delta\boldsymbol{M}_k\boldsymbol{\phi}_j = \delta_{ij} - m_{Bij,k} \quad (\ j \ge i\ ) \tag{7}$$

where δ_{ij} is the Kronecker symbol, when i=j, $\delta_{ij}=1$; when $i \ne j$, $\delta_{ij}=0$.
Expanding Eq. (7) gives:

$$\phi_{1i}\phi_{1j}\Delta m_{1,k} + \phi_{2i}\phi_{2j}\Delta m_{2,k} + \cdots + \phi_{Ni}\phi_{Nj}\Delta m_{N,k} = \delta_{ij} - m_{Bij,k} \tag{8}$$

For the Nth order mode, N(N+1)/2 equations can be obtained, and these equations can be arranged as a set of algebraic equations with $\Delta m_{i,k}$ $(i = 1, 2, \ldots, N)$ as unknowns:

$$\boldsymbol{A}_k\{\Delta m\}_k = \boldsymbol{B}_k \tag{9}$$

in which, $\{\Delta m\}_k$ is a vector made up of main diagonal elements in $\Delta\boldsymbol{M}_k$. The number of equations contained in Eq. (9) is greater than the number of unknowns, and the least squares solution of $\{\Delta m\}_k$ can be expressed as:

$$\{\Delta m\}_k = \left(\boldsymbol{A}_k^T\boldsymbol{A}_k\right)^{-1}\boldsymbol{A}_k^T\boldsymbol{B}_k \tag{10}$$

For the frame structure, if the total mass m_a of the model is known, the sum of the lumped mass should be equal to m_a when the initial mass matrix is assigned; that is,

$$\sum_{i=1}^{N} m_{i,0} = m_a \tag{11}$$

When correcting the mass, the constraint condition is introduced:

$$\sum_{i=1}^{N} \Delta m_{i,k} = 0 \tag{12}$$

Using the Lagrange multiplier method, the optimal equation to solve the minimum value of Eq. (9) under the constraint of Eq. (12) can be expressed as:

$$\begin{aligned} f(\{\Delta m\}_k) = &\{\Delta m\}_k^T\boldsymbol{A}_k^T\boldsymbol{A}_k\{\Delta m\}_k - 2(\boldsymbol{A}_k^T\boldsymbol{B}_k)^T\{\Delta m\}_k \\ &+ (\boldsymbol{A}_k^T\boldsymbol{B}_k)^T(\boldsymbol{A}_k^T\boldsymbol{B}_k) + \alpha\boldsymbol{A}_c^T\{\Delta m\}_k \end{aligned} \tag{13}$$

where α is the Lagrange multiplier; $\boldsymbol{A}_c = \{1 \;\; 1 \;\; \ldots \;\; 1\}^T$ is a vector, whose elements are all unity. Taking the derivative of Eq. (13) with respect to $\{\Delta m\}_k$ and α respectively and setting the corresponding derivative to zero, the system of algebraic equations can be obtained:

$$\begin{bmatrix} 2\boldsymbol{A}_k^T\boldsymbol{A}_k & \boldsymbol{A}_c \\ \boldsymbol{A}_c^T & 0 \end{bmatrix}\begin{Bmatrix} \{\Delta m\}_k \\ \alpha \end{Bmatrix} = \begin{Bmatrix} 2\boldsymbol{A}_k^T\boldsymbol{B}_k \\ 0 \end{Bmatrix} \tag{14}$$

Solving Eq. (14) can get the kth iteration correction of lumped mass that satisfies the constraints.

Due to the errors of the measured modes, it is still impossible to accurately establish Eq. (5) through the correction of the mass matrix. However, the corrected mass can become smaller and smaller through iterative calculation. When the corrected mass is small enough, the iteration can be terminated. The conditions for the termination of the iteration can be expressed as:

$$\frac{\|\Delta\boldsymbol{M}_k\|}{\|\boldsymbol{M}_k\|} < e \tag{15}$$

in which, $\|\Delta\boldsymbol{M}_k\|$ and $\|\boldsymbol{M}_k\|$ are the second-order norms of $\Delta\boldsymbol{M}_k$ and $\boldsymbol{M}_k$ respectively; e is a predetermined tolerance and usually is set to 1×10^{-6}.

3. Least squares solution for lateral stiffness

After obtaining the corrected mass matrix $\boldsymbol{M}$, the jth mode satisfies the eigenvalue equation:

$$\boldsymbol{K}\boldsymbol{\phi}_j = \omega_j^2\boldsymbol{M}\boldsymbol{\phi}_j \tag{16}$$

where ω_j is the jth natural frequency; $\boldsymbol{K}$ is the stiffness matrix of the structure. When all natural frequencies and modes are known, the stiffness matrix can be expressed as:

$$\boldsymbol{K} = \boldsymbol{M}\boldsymbol{\phi}\ diag[\omega_j^2]\boldsymbol{\phi}^T\boldsymbol{M} \tag{17}$$

When the modal and mass matrices have errors, the stiffness matrix obtained by Eq. (17) is a full matrix, which leads to inconsistency between the stiffness matrix and the physical model. In order to make the identified stiffness matrix conform to the physical model, for the lumped-mass shear model, $\boldsymbol{K}$ has to be a tridiagonal matrix. When the numbering method of the degrees of freedom in Fig. 1 is adopted, the relationship between the stiffness matrix $\boldsymbol{K}$ and the lateral stiffness can be expressed as [24]:

$$\boldsymbol{K} = \boldsymbol{TkT}^T \tag{18}$$

where $\boldsymbol{k} = diag[k_i]$ is the diagonal matrix of lateral stiffness; k_i is the lateral stiffness of the ith layer; $\boldsymbol{T}$ is the stiffness transformation matrix:

$$\boldsymbol{T} = \begin{bmatrix} 1 & -1 & 0 & \dots & 0 \\ 0 & 1 & -1 & \dots & 0 \\ \dots & \dots & \dots & \dots & \dots \\ 0 & \dots & \dots & 1 & -1 \\ 0 & \dots & \dots & 0 & 1 \end{bmatrix} \tag{19}$$

Eq. (18) denotes that the stiffness matrix is similar to the diagonal matrix of lateral stiffness for the lumped-mass shear model. After multiplying both sides of Eq. (16) by $\boldsymbol{\phi}_j^T$ on the left, using Eq. (18) and the modal orthogonality relation on the mass matrix, the following equations can be obtained:

$$\boldsymbol{\phi}_i^T \boldsymbol{TkT}^T \boldsymbol{\phi}_j = \lambda_i \, \delta_{ij} \tag{20}$$

Let

$$\boldsymbol{x}_i = \boldsymbol{T}^T \boldsymbol{\phi}_i \tag{21}$$

Expanding Eq. (20) gives:

$$x_{1i} x_{1j} k_1 + x_{2i} x_{2j} k_2 + \cdots + x_{Ni} x_{Nj} k_n = \delta_{ij} \lambda_i \tag{22}$$

After $N(N+1)/2$ numbers of Eq. (22) are taken from the upper triangular part of Eq. (20), these equations can be rewritten in matrix form:

$$\boldsymbol{X}\{k\} = \boldsymbol{Y} \tag{23}$$

in which $\{k\}$ is a vector composed of the main diagonal elements of $\boldsymbol{k}$. Then the least squares solution of $\{k\}$ is:

$$\{k\} = \left(\boldsymbol{X}^T \boldsymbol{X}\right)^{-1} \boldsymbol{X}^T \boldsymbol{Y} \tag{24}$$

From the calculation processes of Eq. (14) and Eq. (24), it can be seen that the prior information of the mass and stiffness of each layer is not required. The identified lumped mass and lateral stiffness is consistent with physical model. And the natural frequency and mode of the structure as well as the total mass are required to solve the lumped mass and lateral stiffness directly so that the calculation is relatively simple.

4. The algorithm workflow

To make the procedure of the algorithm clearer, the workflow of the proposed method is shown in Fig. 2. The algorithm is executed in six steps:

Step 1: Measure the natural frequencies of the model and the corresponding modes $\omega_i, \boldsymbol{\phi}_i$ (i=1,2,…,N).

Step 2: Assume initial lumped mass $m_{i,0}$(i=1,2,…,N) satisfy with Eq. (11), and set k=1.

Step 3: Normalize $\boldsymbol{\phi}_i$ (i=1,2,…,N) by Eq. (3).

Step 4: Assemble the matrix $\boldsymbol{A}_k$ and the vector $\boldsymbol{B}_k$, then obtain $\{\Delta m\}_k$ by Eq. (14), and set $\boldsymbol{M}_{k+1} = \boldsymbol{M}_k + \Delta \boldsymbol{M}_k$.

Step 5: If $\frac{\|\Delta \boldsymbol{M}_k\|}{\|\boldsymbol{M}_k\|} < e$, output the $\boldsymbol{M}_{k+1}$ as the solution and terminate the computation; otherwise, set k=k+1, and go back to Step 3.

Step 6: Assemble the matrix $\boldsymbol{X}$ and the vector $\boldsymbol{Y}$, then obtain $\{k\}$ by Eq. (24).

5. Validation of the proposed algorithm

The following 3-layer steel frame is an example to verify the accuracy and effectiveness of the proposed algorithm. The frame structure model, shown in Fig. 3, was analyzed by Clough and Penzien [25]. The exact mass of each layer is: m_1=10kg, m_2=7.5kg, m_3=5kg. The exact lateral stiffness of each layer is: k_1=1800N/m, k_2=1200N/s, k_3=600N/m.

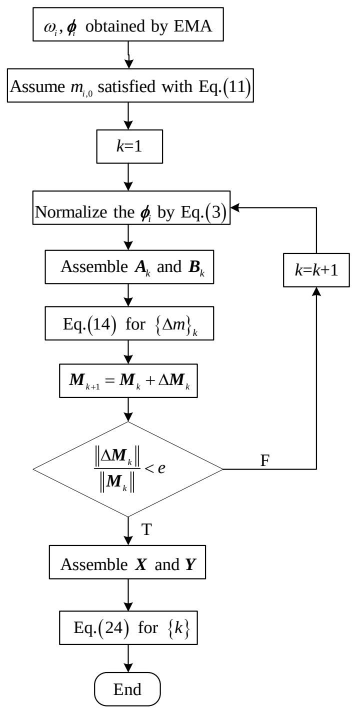

Fig. 2 Flowchart of the proposed method

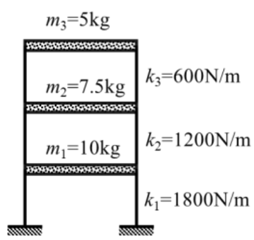

Fig. 3 3-layer steel frame structure model

5.1. Influences of the initial solution on the calculation result

The verification of accuracy and convergence of mass correction in Eq. (14) with the following two initial lumped mass are carried out:

Case 1: $\boldsymbol{M}_0 = diag\begin{bmatrix} 9.5 & 7.5 & 5.5 \end{bmatrix}$

Case 2: $\boldsymbol{M}_0 = diag\begin{bmatrix} 7.5 & 7.5 & 7.5 \end{bmatrix}$

Table 1 shows the lumped mass of each layer after the mass correction of the two cases. Qi [23] used the constrained least squares while Berman [17] used the Lagrange multiplier method for the lumped mass correction. Their results are also listed in the table for comparison.

It is observed that the results of the two cases by the proposed method are the same as the exact solution, while the calculation results by Qi [23] and Berman [17] are different from the exact solution. The relative error e_m of the identified lumped mass can be expressed as:

$$e_m = \frac{m^* - m}{m^*} \times 100\% \tag{25}$$

in which m and m* are the approximate and exact mass respectively.

The maximum relative errors of Case 1 and Case 2 obtained by Qi [23] are 4.72% and 23.28% respectively, and the maximum relative errors of the main diagonal elements of Case 1 and Case 2 obtained by Berman [17] are 3.54% and 17.74% respectively. This shows that the accuracy of the correction by these two methods is related to the initial solution. In these two methods, the smaller the difference between the initial solution and the exact solution, the higher the accuracy of the correction result, and their identified total mass is unequal to the exact solution even if the total mass of the initial solution is consistent with the exact solution.

Table 1
The corrected lumped mass of 3-layer steel frame

Method	Case1	Case2
Present Study	$\begin{bmatrix} 10 & & \\ & 7.5 & \\ & & 5 \end{bmatrix}$	$\begin{bmatrix} 10 & & \\ & 7.5 & \\ & & 5 \end{bmatrix}$
Ref. [23]	$\begin{bmatrix} 9.911 & & \\ & 7.563 & \\ & & 5.236 \end{bmatrix}$	$\begin{bmatrix} 9.379 & & \\ & 7.525 & \\ & & 6.164 \end{bmatrix}$
Ref. [17]	$\begin{bmatrix} 10.016 & 0.226 & 0 \\ 0.226 & 7.597 & -0.004 \\ 0 & -0.004 & 5.177 \end{bmatrix}$	$\begin{bmatrix} 10.081 & 1.129 & 0 \\ 1.129 & 7.984 & 0.565 \\ 0 & 0.565 & 5.887 \end{bmatrix}$

On the contrary, in the proposed method, different initial mass would also converge to the exact solution, which demonstrates good calculation accuracy and stability. Fig. 4 shows the calculation errors obtained in the iterative process of the two cases. From the calculation results, the initial solution would only influence the number of iterative steps, 14 and 16 iteration steps for Case 1 and Case 2 respectively. However, it has no effect on the convergence result.

Table 2 shows the lateral stiffness of each layer obtained from Eq. (24) based on the identified lumped mass. The maximum relative errors of Case 1 and Case 2 stiffness obtained by Qi [23] are 1.50% and 5.75% respectively and by Berman [17] are 3.92% and 19.83% respectively. This result shows that the errors of the identified lateral stiffness by Qi and by Berman would increase with the increase of the error of the identified mass. In the proposed method, the identified lateral stiffness is the same as the exact solution.

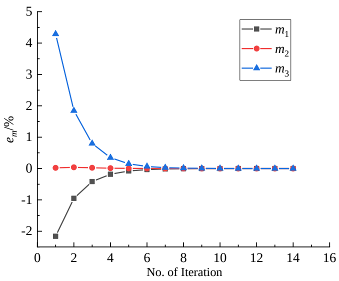

(a) Case 1

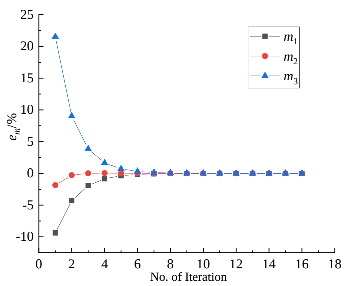

(b) Case 2

Fig. 4 Errors of identified lumped mass in the iterative process

5.2. The influence of the error of measured mode

Error is inevitable in experiment modal analysis (EMA) of engineering structures. Generally, the error of measured mode is much larger than that of measured frequency [6]. Therefore, in the following analysis, the influence of modal measurement error on the identification of the lumped mass and lateral stiffness is investigated, and the error of measured frequency is ignored. It is assumed that the relative error of measured modes is in a normal distribution:

Table 2
Identified lateral stiffness (kN/m)

k_i	Case1			Case2		
	Present study	Ref.[23]	Ref. [17]	Present study	Ref.[23]	Ref. [17]
k_1	1.800	1.824	1.819	1.800	1.884	1.888
k_2	1.200	1.193	1.153	1.200	1.131	0.962
k_3	0.600	0.609	0.609	0.600	0.633	0.640

$$\varepsilon \sim N(0,\sigma^2) \tag{26}$$

in which σ is the standard deviation. The mode with noise after considering the measurement error is:

$$\phi_{ij} = \phi_{ij}^{*}(1+\varepsilon) \tag{27}$$

in which ϕ_{ij}^{*} is the exact value of modal displacement.

In order to analyze the statistical results of the influence of measurement error on the identification of lumped mass and stiffness, 100 groups of random numbers are generated for each standard deviation. Fig. 5 is the box diagram of the lumped mass and stiffness under the standard deviation of 0.01, 0.02, 0.03, 0.04 and 0.05 respectively. Since the proposed method is independent of the initial mass, the convergence result of Case 1 initial mass distribution is the same as that of Case 2. It can be seen from the calculation results that although there is measurement error in the mode, the median value of the identified mass and stiffness are very close to the exact solution. The variance of identification results becomes greater with increasing error of the measured mode. Table 3 shows the errors of the mean value of the identified lumped mass and lateral stiffness under different variances. The numerical results show that the error of mean is less than 1% and is independent of the variation of measured mode.

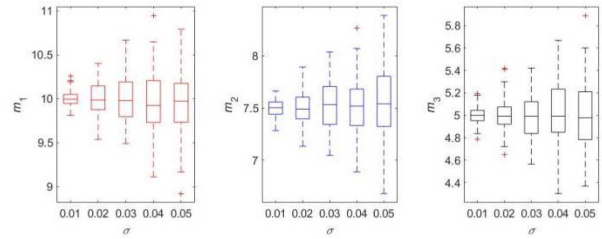

(a) Mass

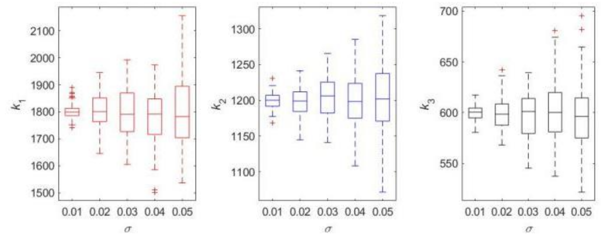

(b) Stiffness

Fig. 5 Box diagram for identifying mass and stiffness under different errors

Table 3
Errors of mean value of identified lumped mass and lateral stiffness (%)

σ	m_1	m_2	m_3	k_1	k_2	k_3
0.01	0.038	-0.055	0.008	0.060	-0.031	-0.022
0.02	-0.003	-0.008	0.017	0.307	-0.119	-0.147
0.03	-0.065	0.265	-0.267	-0.103	0.196	-0.316
0.04	-0.516	0.280	0.611	-0.786	-0.108	0.397
0.05	-0.303	0.595	-0.286	-0.093	0.257	-0.667

To further analyze the influence of the error of measured mode on the calculation results, the coefficients of variation (COV) of identified parameters are defined:

$$\kappa = \frac{\sigma_\xi}{\bar{\xi}} \tag{28}$$

in which σ_ξ and $\bar{\xi}$ are the standard deviation and mean value of variable ξ (m_i and k_i, i=1, 2, 3) respectively. Fig. 6 shows the COV of the identified lumped mass and lateral stiffness under various variances of measured mode. The COV clearly increases with the increase of variance. However, the COV of the mass is almost the same as that of the stiffness. For example, when the standard deviation of mode is 5%, the COV of mass and stiffness are also approximately 5%, which shows that the error of identified lumped mass and lateral stiffness is almost the same as that of mode. The error of measured mode is not enlarged in the process of identifying lumped mass and lateral stiffness in turn, so the identification method has good stability.

6. Mass and stiffness identification of frame test model

To further verify the adaptability of the proposed method in the frame test model, a shear steel frame model is designed. The steel frame is a two-story two-span one-bay structure with layer height of 0.39m, a span of 500mm and a bay of 375mm. The designed section of the column is 4mm × 20mm, the beam is 4mm (width) × 15mm (height), and the floor slab is a 4mm thick steel plate. In order to avoid torsional vibration of the structure, diagonal braces with a cross-section of 4mm × 8mm are installed in the vertical vibration direction. The design weight of the model is 53.2kg. However, due to the thickness imperfection of the steel plates, the actual weight of the test model is 49.2kg. To analyze the lumped mass and lateral stiffness of two degrees of freedom formed by the frame model, three counterweight combinations are applied, as shown in Table 4, which are called Structure 1, Structure 2 and Structure 3 respectively. The photos of the tested steel frames are shown in Fig. 7. The EMA is carried out by the acceleration signal of the accelerometer under the excitation of a force hammer on the second floor. Then the eigensystem realization algorithm (ERA) [28] is used to identify the dynamic characteristics. The identified natural frequencies are shown in Table 5 and the mode shapes are shown in Fig. 8.

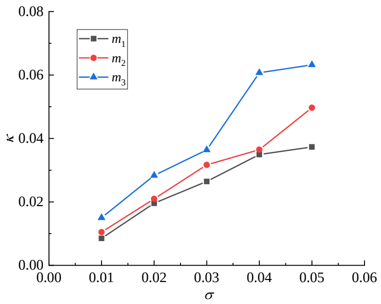

(a) Mass

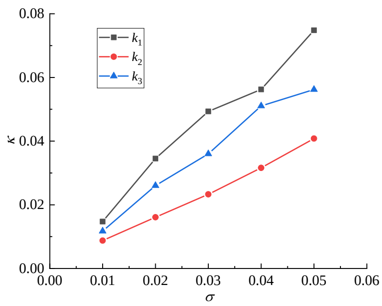

(b) Stiffness

Fig. 6 COV of the identified lumped mass and lateral stiffness

Table 4
Counterweight of structure (kg)

The Floor	Structure 1	Structure 2	Structure 3
1	13.5	27.5	41
2	8.6	22.6	36.1

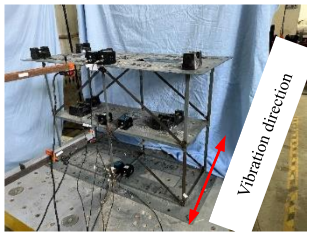

(a) Structure 1

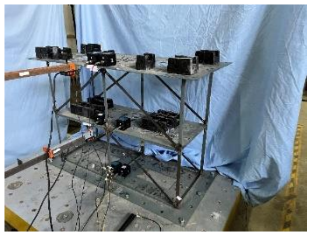

(b) Structure 2

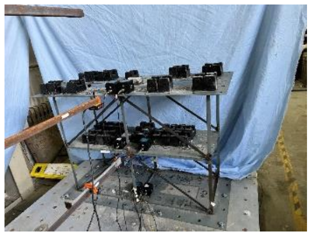

(c) Structure 3

Fig. 7 Photos of tested steel frames

Table 5
Measured natural frequencies (Hz)

No. of Mode	Structure 1	Structure 2	Structure 3
1	2.990	2.380	2.030
2	7.934	6.331	5.420

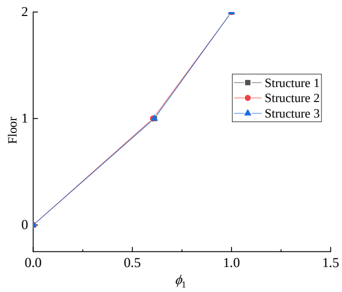

(a) The 1st mode

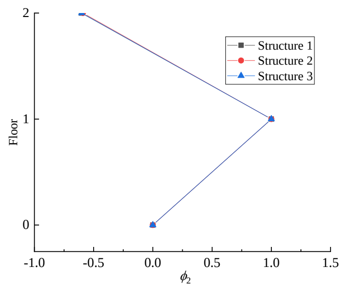

(b) The 2nd mode

Fig. 8 Modes of the structure

According to the measured mass of the frame structure, the total net mass of the two lumped mass of the test models is 31.33kg as the constraint condition. By the proposed method, the lumped mass and lateral stiffness of the three structures are identified, as shown in Table 6.

Table 6
The identified mass and stiffness of the 2-story steel frame

Floor	Structure 1			Structure 2			Structure 3		
	Mass (Kg)	Net mass (Kg)	Lateral stiffness (kN/m)	Mass (Kg)	Net mass (Kg)	Lateral stiffness (kN/m)	Mass (Kg)	Net mass (Kg)	Lateral stiffness (kN/m)
1	26.545	13.045	25.517	40.238	12.738	25.019	53.730	12.730	24.054
2	26.885	18.285	25.176	41.192	18.592	24.239	54.700	18.600	23.842

The net mass in Table 6 is the identified lumped mass minus the counterweight, which means the lumped mass of the test model. The maximum difference of the identified net mass of the three structures is 2.41%. The difference in the identification results of different counterweights is caused by random errors in the measured mode. The maximum difference of the identified lateral stiffness is 5.73%, which is slightly greater than that of the lumped mass. This is also caused by some random errors of the measured natural frequency. Based on the identified lumped mass and lateral stiffness, the analytical natural frequencies of the three structures are estimated by eigenvalue analysis, as shown in Table 7.

If the natural frequency obtained from the test is taken as the accurate solution, the relative error of the analytical natural frequencies can then be defined by:

$$e_\omega = \frac{\omega_j - \omega_j^*}{\omega_j^*} \times 100\% \tag{29}$$

in which ω_j and ω_j^* are the analytical and measured natural frequencies respectively. The relative error of the analytical natural frequency is shown in Table 8. The calculation result shows that the maximum error of analytical natural frequency is 1.72%, which shows good accuracy of the identified lumped mass and lateral stiffness.

Table 7
Analytical natural frequencies of the 2-story steel frame(Hz)

No. of Mode	Structure 1	Structure 2	Structure 3
1	3.030	2.421	2.065
2	7.932	6.329	5.418

Table 8
Relative errors (%) of analytical natural frequency of the 2-story steel frame

No. of Mode	Structure 1	Structure 2	Structure 3
1	1.338	1.723	1.724
2	-0.025	-0.032	-0.037

7. Conclusion

To identify the mass matrix and stiffness matrix of the shear-type frame test model, a high precision identification method is proposed to correct the lumped mass and lateral stiffness based on the natural frequencies and modes. According to the analytical and experimental results, the following conclusions can be drawn:

(1) For the shear-type frame structure, the lumped mass is a diagonal matrix, and the stiffness matrix can also be transformed into a diagonal matrix of lateral stiffness by the stiffness transformation matrix. The iterative constrained optimization solution of the mass matrix correction and the least squares solution of the lateral stiffness are established. Therefore, the identified mass matrix and stiffness matrix have clear physical significance.

(2) The identified mass matrix is independent of the initial mass and does not demand the prior mass distribution. When the measured modes are exact, the identified mass converges to the exact solution. When there are errors in the measured modes, the error of the identified lumped mass and lateral stiffness is almost the same as the modal error. The modal error does not enlarge in the process of identifying the lumped mass and lateral stiffness in turn, and the identification method has good stability.

(3) The maximum differences of identified lumped mass and lateral stiffness of steel frame test model with three different counterweights are 2.41% and 5.73% respectively. The maximum error between the analytical and experimental natural frequencies is 1.72%, which shows a good accuracy.

The identification method of stiffness coefficients in this paper is applicable to shear-type frame structures whose stiffness matrix is a tridiagonal matrix. In the future, more research is needed to identify the physical parameters of the bending-type structures.

References

[1] G. Q. Li, J. Z. Zhang, L. L. Li, et al., "Progressive collapse resistance of steel framed buildings under extreme events", Advanced Steel Construction, Vol. 17, pp. 318-330, 2021. Doi: 10.18057/IJASC.2021.17.3.10
[2] A. L. Zhang, G. H. Shangguan, Y. X. Zhang, et al., "Experimental study of resilient prefabricated steel frame with all-bolted beam-to-column connections", Advanced Steel Construction, Vol. 16, pp. 255-271, 2020. Doi: 10.18057/IJASC.2020.16.3.7
[3] J. P. Yang, P. Z. Li, Z. Lu., "Large-scale shaking table test on pile-soil-structure interaction on soft soils", The Structural Design of Tall and Special Buildings, Vol. 28, pp. 1679, 2019. Doi: 10.1002/tal.1679
[4] Q. Wang, J. T. Wang, F. Jin, et al., "Real-time dynamic hybrid testing for soil–structure interaction analysis", Soil Dynamics and Earthquake Engineering, Vol. 31, pp. 1690-1702, 2011. Doi: 10.1016/j.soildyn.2011.07.004
[5] K.S. Al-Jabri, S. M. Al-Alawi, A. H. Al-Saidy, et al., "An artificial neural network model for predicting the behaviour of semi-rigid joints in fire", Advanced Steel Construction, Vol. 5, pp. 452-464, 2009.
[6] J. E. Mottershead, M. I. Friswell., "Model updating in structural dynamics: A survey", Journal of Sound and Vibration, Vol. 167, pp. 347-375, 1993. Doi: 10.1006/jsvi.1993.1340
[7] X. Zhou, Y. Xia, S. Weng., "L1 regularization approach to structural damage detection using frequency data", Structural Health Monitoring, Vol. 14, pp. 571-582, 2015. Doi: 10.1177/1475921715604386
[8] W. X. Ren, H. B. Chen., "Finite element model updating in structural dynamics by using the response surface method", Engineering Structures, Vol. 32, pp. 2455-2465, 2010. Doi: 10.1016/j.engstruct.2010.04.019
[9] Y. F. Xu, W. D. Zhu, S. A. Smith., "Non-model-based damage identification of plates using principal, mean and Gaussian curvature mode shapes", Journal of Sound and Vibration, Vol. 400, pp. 626-659, 2021. Doi: 10.1016/j.jsv.2017.03.030
[10] A. K. Panda, S. V. Modak., "An FRF-based perturbation approach for stochastic updating of mass, stiffness and damping matrices", Mechanical Systems and Signal Processing, Vol. 166, pp. 108416, 2022. Doi: 10.1016/j.ymssp.2021.108416
[11] S. Pradhan, S. V. Modak., "A two-stage approach to updating of mass, stiffness and damping matrices", International Journal of Mechanics Sciences, Vol. 140, pp. 133-150, 2018. Doi: 10.1016/j.ijmecsci.2018.02.033
[12] X. G. Li, F. S. Liu., "A nonmode-shape-based model updating method for offshore structures using extracted components from measured accelerations", Applied Ocean Research, Vol. 121, pp. 103087, 2022. Doi: 10.1016/j.apor.2022.103087
[13] J. E. Mottershead, M. Link, M. I. Friswell., "The sensitivity method in finite element model updating: A tutorial", Mechanical Systems and Signal Processing, Vol. 25, pp. 2275-2296, 2011. Doi: 10.1016/j.ymssp.2010.10.012
[14] V. Alves, M. Oliveira, D. Ribeiro, et al., "Model-based damage identification of railway bridges using genetic algorithms", Engineering Failure Analysis, Vol. 118, pp. 104845, 2020. Doi: 10.1016/j.engfailanal.2020.104845
[15] H. Y. Gou, T. Q. Zhao, S. Q. Qin, et al., "In-situ testing and model updating of a long-span cable-stayed railway bridge with hybrid girders subjected to a running train", Engineering Structures, Vol. 253, pp. 113823, 2022. Doi: 10.1016/j.engstruct.2021.113823
[16] R. Ghanem, M. Shinozuka., "Structural system identification. I: Theory", Journal of Engineering Mechanics, Vol. 121, pp. 255-264, 1995. Doi: 10.1061/(ASCE)0733-9399(1995)121:2(255)
[17] A Berman., "Mass matrix correction using an incomplete set of measured modes", AIAA Journal, Vol. 17, pp. 1147-1148, 1979. Doi: 10.2514/3.61290
[18] P. Jack, T. P. Holman, M. Mott-Smith, et al., "Optimal correction of mass and stiffness matrices using measured modes", AIAA Journal, Vol. 20, pp. 1623-1626, 1982. Doi: 10.2514/3.7995
[19] F.S. Wei., "Analytical dynamic model improvement using vibration test data", AIAA Journal, Vol. 28, pp. 175-177, 1990. Doi: 10.2514/3.10371
[20] F.S. Wei., "Mass and stiffness interaction effects in analytical model modification", AIAA Journal. Vol. 28, pp. 1686-1688, 1990. Doi: 10.2514/3.25269
[21] E. T. Lee, H. C. Eun., "Correction of stiffness and mass matrices utilizing simulated measured modal data", Applied Mathematical Modelling, Vol. 33, pp. 2723-2729, 2009. Doi: 10.1016/j.apm.2008.08.010
[22] E. T. Lee, H. C. Eun., "Update of corrected stiffness and mass matrices based on measured dynamic modal data", Applied Mathematical Modelling, Vol. 33, pp. 2274-2281, 2009. Doi: 10.1016/j.apm.2008.06.004
[23] W. R. Qi., "Damping model and seismic response analysis of frame structures", University of Science and Technology Beijing, 2021. (in Chinese)
[24] G. L. Gladwell., "Inverse problems in vibration", Springer Netherlands, Waterloo, Ontario, Canada, 2005.
[25] R. W. Clough, J Penzien. "Dynamics of structures", 2nd Edition, Computers and structures, Inc., Berkeley, CA, USA, 1995.

[26] G. B. Wang, Y. Wang, H. T. Yu, et al., "Shaking table tests on seismic response of rocking frame structure considering foundation uplift", Chinese Journal of Geotechnical Engineering, Vol. 43, pp. 2064-2074, 2021. Doi:10.13374/j.issn1001-053x.2014.12.020 (in Chinese)
[27] D. G. PAN, L. L. Gao., G. H. Jin, et al., "Model test of dynamic characteristics of structure-soil-structure system", Journal of University of Science and Technology Beijing, Vol. 36, pp. 1720-1728, 2014. Doi: 10.13374/j.issn1001-053x.2014.12.020 (in Chinese)
[28] J. N. Juang, R. S. Pappa. "An eigensystem realization algorithm for modal parameter identification and model reduction". Journal of Guidance, Control, and Dynamics, vol. 8, pp. 620-627. 1985. Doi:10.2514/3.20031